

# Sandpile model on Scale Free Networks with preferential sand distribution: a new universality class

Himangsu Bhaumik and S. B. Santra\*

*Department of Physics, Indian Institute of Technology Guwahati, Guwahati-781039, Assam, India.*

(Dated: September 30, 2018)

A two state sandpile model with preferential sand distribution is developed and studied numerically on scale free networks with power-law degree ( $k$ ) distribution, *i.e.*:  $P_k \sim k^{-\alpha}$ . In this model, upon toppling of a critical node sand grains are given one to each of the neighbouring nodes with highest and lowest degrees instead of two randomly selected neighbouring nodes as in a stochastic sandpile model. The critical behaviour of the model is determined by characterizing various avalanche properties at the steady state varying the network structure from scale free to random, tuning  $\alpha$  from 2 to 5. The model exhibits mean field scaling on the random networks,  $\alpha > 4$ . However, in the scale free regime,  $2 < \alpha < 4$ , the scaling behaviour of the model not only deviates from the mean-field scaling but also the exponents describing the scaling behaviour are found to decrease continuously as  $\alpha$  decreases. In this regime, the critical exponents of the present model are found to be different from those of the two state stochastic sandpile model on similar networks. The preferential sand distribution thus has non-trivial effects on the sandpile dynamics which leads the model to a new universality class.

PACS numbers: 89.75.-k,64.60.aq,05.65.+b,64.60.av

## I. INTRODUCTION

The degree distribution  $P_k$ , probability to have a node with degree  $k$ , of a class of complex networks [1, 2] is given by

$$P_k \sim k^{-\alpha} \quad (1)$$

where  $\alpha$  is the characteristic degree exponent. Such networks are known as scale-free network (SFN) [3]. The behaviour of many systems like epidemic spreading [4, 5], percolation [6], etc. occurring on the SFN have strong dependence on  $\alpha$  because of diverging moment of degree distribution;  $\langle k^n \rangle \rightarrow \infty$  for  $n \geq \alpha - 1$  as  $k_{\max}$  is infinitely large. Depending upon the value of  $\alpha$  the network has two regimes scale free and random. The scale free regime,  $2 \leq \alpha \leq 3$ , is characterized by finite average degree  $\langle k \rangle$  and diverging second moment of the degree distribution  $\langle k^2 \rangle$  whereas in the random regime both are found to be finite [7]. Furthermore, due to strong heterogeneity in the degree distribution, the translational symmetry, nodes with similar neighbourhood, is absent in the scale free regime whereas it is a necessary condition in the random regime [8]. The percolation model [6] as well as the epidemic spreading model [9] exhibits mean-field (MF) behaviour on random network for  $\alpha > 4$  whereas shows some non-trivial critical behaviour other than MF on scale free network for  $\alpha < 4$ . On the other hand, due to the heterogeneity in degrees, SFN with  $\alpha \leq 3$  are highly resilience against random attack [10] whereas it is vulnerable when the attack is targeted on a few nodes with larger degree [11]. Under such intentional attack a devastating cascading failure such as black out of electric

power grid in an entire country could happen through out a network [12, 13].

Avalanche dynamics of a sandpile model [14–16] manifests such cascading effects where the system in the critical state is triggered by a small perturbation and the response spreads all over the system redistributing sand (or energy) in a cascaded manner. Various types of sandpile models in Euclidean space have been studied introducing different kinds of constraints in the sand distribution dynamics via well defined toppling rules such as stochastic [17], directional [18], rotational [19] etc. In all such cases, the models are found to belong to different universality classes. Both Bak Tang Wiesenfeld (BTW) sandpile model [20, 21] and stochastic sandpile model (SSM) [17] have been introduced on SFN [22, 23]. Though the avalanche size distribution is highly affected by  $\alpha$  in the BTW model, it represents MF behaviour for the SSM for all values of  $\alpha \geq 2$ . However, to our knowledge, sandpile model on SFN with targeted sand distribution to nodes with specific degrees is still not reported. Since the targeted sand distribution in certain models leads to non-trivial scaling behaviour, it is intriguing to develop a sandpile model on SFN distributing sand to nodes with specific degrees and study the sandpile dynamics on varied scale free structures.

In this paper, a two state sandpile model with preferential sand distribution, in short a preferential sandpile model (PSM), is developed and studied on SFN varying the degree exponent  $\alpha$ . In the preferential rule, sands are given to the highest and the lowest degree neighbouring nodes in the event of toppling of a critical node. The model represents nontrivial critical behaviour for  $\alpha < 4$  and MF behaviour for  $\alpha > 4$  as seen in the epidemic spreading model on SFN [9]. Results are compared with those of the SSM, a two state stochastic sandpile model, on SFN [22].

---

\* santra@iitg.ac.in

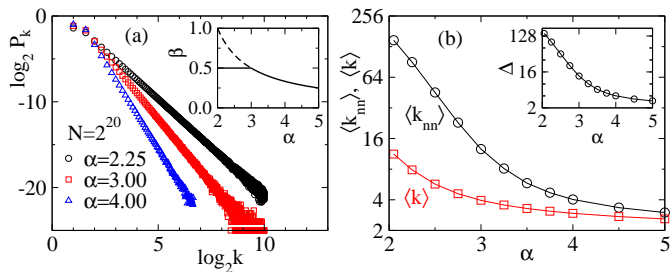


FIG. 1. (Colour online) (a) Plot of  $P_k$  against  $k$  for different values of  $\alpha$  for a network of size  $N = 2^{20}$ . The distribution is sampled over 32 configurations. Inset: Plot of  $\beta = \ln k_{\max} / \ln N$  vs  $\alpha$  shown in solid line. The dashed line shows the natural cutoff  $\beta = 1/(\alpha - 1)$  for  $\alpha < 3$ . (b) Plot of  $\langle k_{nn} \rangle$  ( $\circ$ ) and  $\langle k \rangle$  ( $\square$ ) against  $\alpha$ . Inset shows how their difference  $\Delta = \langle k_{nn} \rangle - \langle k \rangle$  changes with  $\alpha$ .

## II. THE MODEL

Scale free networks of  $N$  nodes are generated employing uncorrelated configurational model [24]. In order to get a scale-free degree distribution, a random number  $r$ , uniformly distributed between  $[0, 1]$ , is drawn for each node and degree  $k = \text{INT}[k_{\min}/r^{1/(\alpha-1)}]$  where  $k_{\min} = 2$ , is assigned. The natural upper cutoff of the degree for a SFN is  $k_{\max} = N^\beta$  where  $\beta = 1/(\alpha - 1)$ . However, for  $\alpha \leq 3$  the upper cutoff is set to  $\sqrt{N}$  instead of the natural cutoff which eventually would satisfy the conditions of no multi-edge or self-edge of the nodes in a uncorrelated random SFN. The degree distributions of some of the networks considered are shown in Fig. 1(a) for different values of  $\alpha$ . The values of  $\beta$  used to fix  $k_{\max}$  for different values of  $\alpha$  are shown in the inset of Fig. 1(a). The likely neighbourhood of nodes is identified by comparing the average nearest neighbour degree  $\langle k_{nn} \rangle$  with the average degree  $\langle k \rangle$  of a network as shown in Fig. 1(b). The difference between the two averages  $\Delta = \langle k_{nn} \rangle - \langle k \rangle$  is shown in the inset of Fig. 1(b) and found to be quite large for small  $\alpha$  and decreases to  $k_{\min}$  as  $\alpha \rightarrow \infty$ .

In order to implement sandpile model on a network where there is no boundary, one needs to have an estimate for the rate of dissipation of sand grains during its flow over the network. Bulk dissipation is one of the options in which a sand grain is removed from the system with a small probability  $\epsilon$  during the transfer of a sand grain from one node to another. For given  $\alpha$  and  $\epsilon$ , the SFN with  $N$  nodes is driven by adding sand grains, one at a time, to a randomly chosen node  $i$ . If the height  $h$  of the sand column at the  $i$ th node is greater than or equal to the threshold value  $h_c = 2$ , the sand column becomes unstable or critical and collapses by distributing two sand grains to the neighbouring nodes with the highest and lowest degree among the  $k_i$  adjacent nodes. If more than one node has the same highest (or lowest) degree, one of them is chosen randomly to consider as the highest (or the lowest) degree node. Such special situations are demonstrated in Fig. 2. The toppling rule of

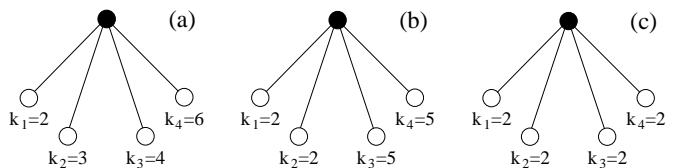


FIG. 2. Toppling rules for PSM on a node of degree  $k = 4$  are demonstrated. The black filled circle represents the critical node which has 4 adjacent nodes (open circle) with degree, say,  $k_1, k_2, k_3$ , and  $k_4$ . In (a)  $k_1 < k_2 < k_3 < k_4$ , the nodes with degree  $k_1$  and  $k_4$  receive one sand grain each. In (b)  $k_1 = k_2 < k_3 = k_4$ , two sand grains are distributed among one of the randomly chosen node from  $\{k_1, k_2\}$  and another from  $\{k_3, k_4\}$ . In (c)  $k_1 = k_2 = k_3 = k_4$ , two sand grains are randomly given to any two distinct nodes.

the  $i$ th critical node of an SFN is then given by

$$h_i \rightarrow h_i - h_c, \quad \text{and} \quad h_j = \begin{cases} h_j & \text{if } r \leq \epsilon, \\ h_j + 1 & \text{otherwise} \end{cases} \quad (2)$$

where  $j$  corresponds to the adjacent nodes with highest and lowest degree,  $r$  is a random number uniformly distributed over  $[0, 1]$ . If the toppling causes any of adjacent nodes critical, subsequent toppling follow on these nodes in parallel until all the nodes in the network become under critical. These toppling activities lead to an avalanche. As an avalanche seized, another sand grain is added to the system.

The model is studied varying  $\alpha$  from 2 to 5 for a given  $\epsilon$ . Since on the random network,  $\epsilon \sim 1/\sqrt{N}$  [25] for a network of  $N$  nodes, the dissipation factor  $\epsilon = 1/\sqrt{N}$  is taken for most of the values of  $\alpha$  and the effect of  $\epsilon$  on the sandpile dynamics is verified for a few specific values of  $\alpha$ .

## III. NUMERICAL SIMULATION

An extensive computer simulation is performed varying  $\alpha$  from 2 to 5. For a given  $\alpha$ , the size of the networks  $N$  varied from  $N = 2^{16}$  to  $N = 2^{20}$  in multiple of 2. In order to estimate the avalanche properties, the following statistical averages are made. For a given  $\alpha$  and  $N$ , thirty two different SFN configurations are considered. On each SFN,  $10^6$  avalanches are collected neglecting the first  $3 \times 10^6$  avalanches during which steady state has been achieved in all networks. Therefore, for a given  $\alpha$  and  $N$ , a total of  $32 \times 10^6$  avalanches is taken for data averaging. The critical behavior of different avalanche properties like the toppling size  $s$  (total number of toppling in an avalanche), area  $a$  (the number of distinct nodes toppled in an avalanche), and lifetime  $t$  (the number of parallel updates to make all the nodes under critical) of an avalanche are measured in the steady state to characterize the PSM on SFN.

The steady state corresponds to balance of incoming and outgoing fluxes of sand grains which leads to time

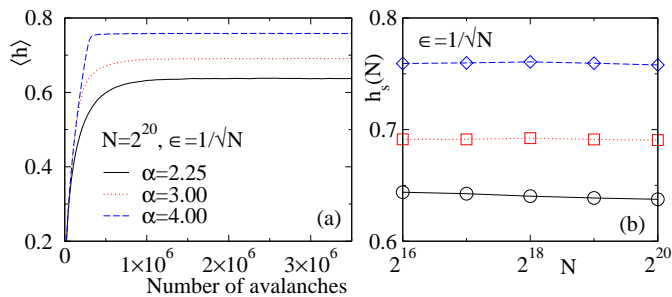


FIG. 3. (Colour online) (a) Plot of  $\langle h \rangle$  against number of avalanches on SFN of size  $N = 2^{20}$  for  $\alpha = 2.25$  (black solid line), 3 (red dotted line), and 4 (blue dashed line) taking  $\epsilon = 1/\sqrt{N}$ . (b) The variation of  $h_s$  with network size  $N$  for  $\alpha = 2.25$  ( $\circ$ ), 3 ( $\square$ ), and 4 ( $\diamond$ ) for the same value of  $\epsilon$ .

independent average height of the sand columns in the network. For a given  $\alpha$ , the average height  $\langle h \rangle$  is calculated as

$$\langle h \rangle = \frac{1}{N} \sum_{i=1}^N h_i \quad (3)$$

where  $h_i$  is the height of the sand column at the  $i$ th node and  $N$  is the total number of nodes in the network. In Fig. 3(a),  $\langle h \rangle$  is plotted against the number of avalanches for different values of  $\alpha$  on a network of size  $N = 2^{20}$ . Starting from an empty configuration, the steady state of PSM is achieved after more than  $10^6$  avalanches for all values of  $\alpha$ . It can be seen that the values of  $\langle h \rangle$  at the steady state increases as  $\alpha$  increases. Since the critical height  $h_c = 2$  in this model, at the end of an avalanche, the nodes either will have a sand or they will remain empty. Thus for  $\alpha = 4$ , nearly 75% of the nodes are having sands whereas for  $\alpha = 2.25$ , nearly 60% of the nodes are having sands. For a given value of  $\alpha$ , the saturated average height  $h_s$  of the sand columns in the steady state is estimated taking average over last  $10^5$  avalanches of every 32 different configurations. For a given value of  $\alpha$ ,  $h_s$  is found to be independent of network size  $N$  as shown in the Fig. 3(b) for three different values of  $\alpha$ . It has also been verified that  $h_s$  increases if the dissipation factor  $\epsilon$  decreases and vice versa for a given  $\alpha$  as expected.

In order to compare the results of PSM with that of the SSM, the above numerical computation has also been repeated for SSM on the similar networks. In case of the SSM, similar variations  $h_s$  with  $\alpha$ ,  $N$  and  $\epsilon$  are observed.

#### IV. AVALANCHE EVOLUTION

Time evolution of a few typical avalanches of PSM generated on a network of size  $N = 2^{14}$  are shown in the upper row of Fig. 4 for different values of  $\alpha$ . For comparison, time evolved morphology of avalanches in the SSM on the same networks are given in the lower row of Fig.

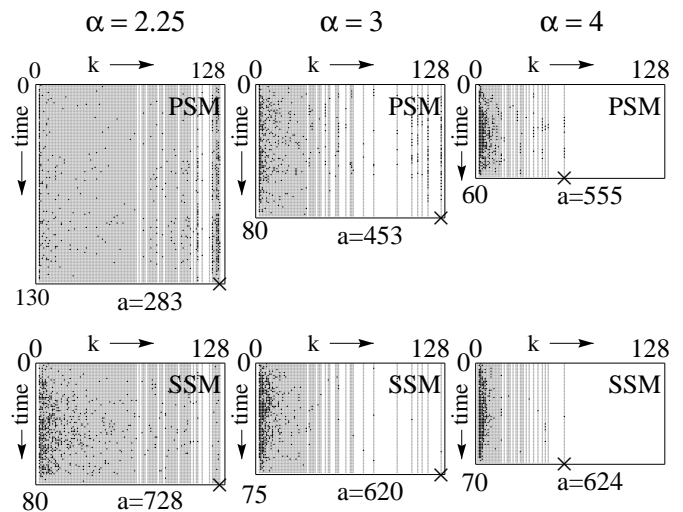


FIG. 4. Time evolution of typical avalanches of PSM (upper row) and those of SSM (lower row) in degree space are shown for  $\alpha = 2.25$  (left column),  $\alpha = 3$  (middle column), and,  $\alpha = 4$  (right column) on a network of size  $N = 2^{14}$  taking  $\epsilon = 1/\sqrt{N}$ . The black dots represent the toppled nodes and the gray colour represents the nodes with no toppling. The white space corresponds to no nodes of such degree. The crosses represent the maximum degree present in the network.

4. The degree  $k$  of the nodes is presented along the horizontal axis and time (the parallel updates) is presented along the downward vertical axis. The black dots represent the toppled nodes, the gray color corresponds to the nodes of certain degree with no toppling and white space corresponds to no node of that degree. The avalanches presented here have a common size  $s = 800$  for both the models, the area  $a$  are mentioned at the bottom of each configuration and their lifetime  $t$  (maximum number of parallel updates) can be seen from the vertical axis. The time evolution of an avalanche of PSM differs considerably than that of SSM on a given network. For PSM,  $a$  increases and  $t$  decreases as  $\alpha$  increases whereas for SSM both  $t$  and  $a$  remains almost same for all values of  $\alpha$ . In PSM, small  $a$  and large  $t$  for smaller  $\alpha$ , indicates multiple toppling of the nodes in the scale free regime ( $2 \leq \alpha \leq 3$ ). On the other hand, in the random regime with  $\alpha \geq 4$ , large  $a$  and small  $t$  indicate single toppling of different nodes. It can also be noted that in PSM the density of toppled nodes is high at the lower and higher degree nodes of the network in scale-free regime whereas most of the lower degree nodes are involved in an avalanche in the random regime. However, in SSM the density of toppled nodes always decreases with  $k$ . The characteristic features of the two models are quite different and hence it is important to characterize the critical avalanche properties of PSM quantitatively and compare the results with those of the SSM on SFN.

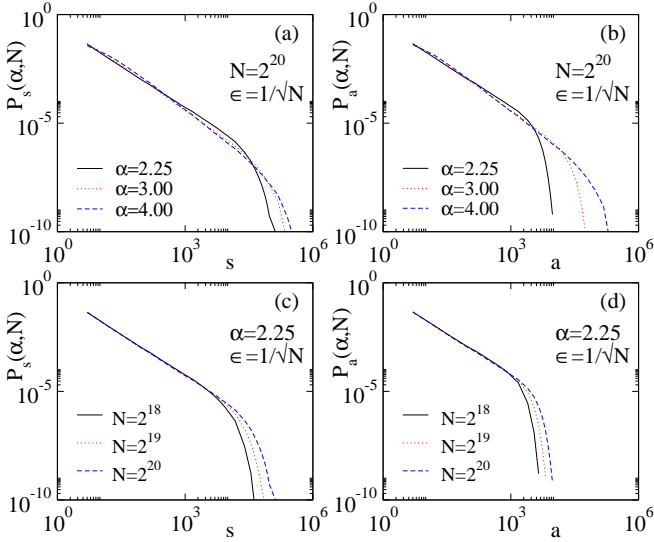


FIG. 5. (Colour online) Plot of  $P_s(\alpha, N)$  against  $s$  and  $P_a(\alpha, N)$  against  $a$  in (a) and (b) respectively for  $\alpha = 2.25$  (solid line),  $\alpha = 3$  (dotted line),  $\alpha = 4$  (dashed line) for a network of size  $N = 2^{20}$ . For a given  $\alpha$ , the distributions for different network sizes  $N = 2^{18}$  (solid line),  $N = 2^{19}$  (dotted line), and  $N = 2^{20}$  (dashed line) are shown in (c) for  $P_s(\alpha, N)$  and in (d) for  $P_a(\alpha, N)$ . All distributions are estimated taking  $\epsilon = 1/\sqrt{N}$ .

## V. CHARACTERIZATION OF PSM ON SFN

To characterize the properties of PSM, the probability distributions  $P_x(\alpha, N)$  of avalanche properties  $x \in \{s, a\}$  at the critical steady state are determined for various values of degree exponent  $\alpha$ , dissipation factor  $\epsilon$  and network size  $N$ . Distributions will be studied taking  $\epsilon = 1/\sqrt{N}$  and the effect of  $\epsilon$  on the distributions will be analyzed later for a specific value of  $\alpha$ . For a fixed  $N = 2^{20}$ , the distributions  $P_s(\alpha, N)$  and  $P_a(\alpha, N)$  are plotted in Figs. 5(a) and 5(b) respectively for several values of  $\alpha$ . Keeping  $\alpha$  fixed at 2.25, the same distributions  $P_s(\alpha, N)$  and  $P_a(\alpha, N)$  for different values of  $N$  are plotted in Figs. 5(c) and 5(d) respectively. Though the cutoffs depend on both  $N$  and  $\alpha$  for a given  $\epsilon$ , the scaling exponents seem to be independent of the network size  $N$  for a given  $\alpha$  but it depends on  $\alpha$  for a given  $N$ . Hence, for given  $\alpha$  and  $N$ , a finite size scaling (FSS) form of  $P_x(\alpha, N)$  is assumed as

$$P_x(\alpha, N) = x^{-\tau_x(\alpha)} f_{x,\alpha} \left[ \frac{x}{N D_x(\alpha)} \right], \quad (4)$$

where  $\tau_x(\alpha)$  is the scaling exponent,  $D_x(\alpha)$  is the capacity dimension, and  $f_{x,\alpha}$  is a  $\alpha$  dependent scaling function of an avalanche property  $x$  for a given  $\epsilon$ . Two important aspects of the distributions need to be verified. First is the universality, *i.e.* determination of the values of the exponents and second is the verification of the FSS form assumed. Though the two state models like SSM [26, 27] and rotational sandpile model [19] follow FSS on regular

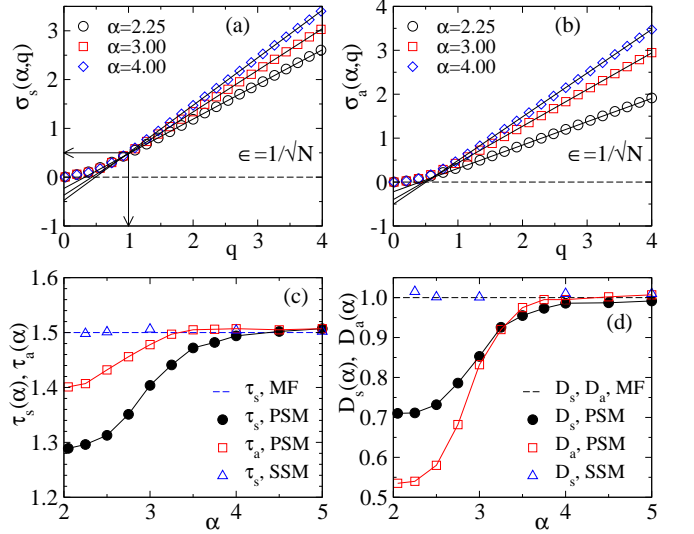


FIG. 6. (Colour online) Plot of (a)  $\sigma_s(\alpha, q)$  and (b)  $\sigma_a(\alpha, q)$  against  $q$  for  $\alpha = 2.25$  ( $\circ$ ),  $\alpha = 3$  ( $\square$ ), and  $\alpha = 4$  ( $\diamond$ ). For clarity only 25 points out of 400 points are shown. The solid lines represent the linear least square fit through the data points. (c) Plot of  $\tau_s(\alpha)$  (black filled circle) and  $\tau_a(\alpha)$  (red open square) against  $\alpha$ . For comparison,  $\tau_s(\alpha) = \tau_a(\alpha)$  for SSM are given in blue triangles. (d) Plot of  $D_s(\alpha)$  (black filled circle) and  $D_a(\alpha)$  (red open square) against  $\alpha$ . The values of  $D_s(\alpha) = D_a(\alpha)$  for SSM are shown in blue triangles. The dashed lines in (c) and (d) represents the MF value. The error in the values of the exponents are of the order of symbol size.

lattice, the BTW model does not. It is then intriguing to verify whether FSS of PSM on SFN is valid or not.

In order to estimate the values of the exponents  $\tau_x(\alpha)$  and  $D_x(\alpha)$ , [Eq. (4)], the concept of moment analysis [28] has been used. For a given  $\alpha$ , the  $q$ th moment of  $x$  as function of  $N$  can be obtained as

$$\langle x^q(\alpha, N) \rangle = \int_0^\infty x^q P_x(\alpha, N) dx \sim N^{\sigma_x(\alpha, q)}, \quad (5)$$

where the  $q$ th moment scaling exponent

$$\sigma_x(\alpha, q) = D_x(\alpha)q + D_x(\alpha)[1 - \tau_x(\alpha)] \quad (6)$$

for  $q > \tau_x(\alpha) - 1$  and it is zero for  $q < \tau_x(\alpha) - 1$ . For each value of  $\alpha$ , a sequence of values of  $\sigma_x(\alpha, q)$  as a function of  $q$  is determined by estimating the slope of the plots of  $\log \langle x^q(\alpha, N) \rangle$  versus  $\log(N)$  for 400 equidistant values of  $q$  between 0 and 4.  $\sigma_s(\alpha, q)$  and  $\sigma_a(\alpha, q)$  are plotted against  $q$  for  $\alpha = 2.25, 3$ , and 4 in Figs. 6(a) and 6(b) respectively. First, it can be seen that for  $q = 1$ , the value of  $\sigma_s(\alpha, 1)$  is found to be  $\approx 1/2$  (indicated by arrows in Fig. 6(a)) irrespective of the values of  $\alpha$ . Since the dissipation factor is taken as  $\epsilon = 1/\sqrt{N}$  for all values of  $\alpha$ , the average number of toppling required for an avalanche to dissipate one sand grain is  $\sqrt{N}$ . Hence,  $\langle s \rangle \sim N^{1/2}$ , *i.e.*  $\sigma_s(\alpha, 1) = 1/2$  for all  $\alpha$ . In order to estimate the values of the exponents, the direct method developed by Lübeck [28] is

employed. Following such method, straight lines are fitted through the data points  $\{\sigma_x(\alpha, q)\}$  in the range of  $2 \leq q \leq 4$  and the exponents  $\tau_x(\alpha)$  and  $D_x(\alpha)$  are obtained from the intercepts on the  $q$ -axis and  $\sigma_x(\alpha, q)$  axis respectively for a given  $\alpha$ . Following Eq. (6), the  $q$  intercept provides  $\tau_x(\alpha) - 1$ , the  $\sigma_x(\alpha, q)$  intercept provides  $D_x(\alpha)[1 - \tau_x(\alpha)]$ . The estimated values of the exponents are:  $\tau_s = 1.296(7)$ ,  $\tau_a = 1.407(6)$ ,  $D_s = 0.720(6)$ ,  $D_a = 0.534(5)$  for  $\alpha = 2.25$ ;  $\tau_s = 1.403(6)$ ,  $\tau_a = 1.478(6)$ ,  $D_s = 0.852(5)$ ,  $D_a = 0.837(6)$  for  $\alpha = 3$ ;  $\tau_s = 1.491(5)$ ,  $\tau_a = 1.503(4)$ ,  $D_s = 0.975(6)$ ,  $D_a = 0.994(5)$  for  $\alpha = 4$ . The number in the parentheses is the uncertainty of last digit in the numerical value of the respective exponents. The values of  $\tau_x(\alpha)$  and  $D_x(\alpha)$  are estimated at various different values of  $\alpha$  and presented as a function of  $\alpha$  in Figs. 6(c) and 6(d) respectively.

In order to compare the values of the exponents of PSM with those of the SSM, the estimates of the values of these exponents for the SSM are also presented in the same figures. The estimated exponents are not only found to be the same as reported in [22] but also same as that of MF [29, 30]. It is already reported that the SSM exhibits MF behaviour [22] throughout the range of  $\alpha$ , scale free as well as random. It is also known that the SSM has a different scaling behaviour than MF on SWN [31] in contrary to the present observation. It is worth mentioning here that for BTW type deterministic sandpile model on SFN, the exponent  $\tau_s(\alpha)$  also has a continuous dependence on  $\alpha$  as  $\tau_s(\alpha) = \alpha/(\alpha - 1) > 3/2$  in the range  $2 < \alpha < 3$  and remains  $\tau_s(\alpha) = 3/2$  for  $\alpha > 3$  [22]. However, in PSM, all four exponents,  $\tau_s$ ,  $\tau_a$ ,  $D_s$ ,  $D_a$ , have MF values in the random regime ( $\alpha \geq 4$ ) but they vary continuously with  $\alpha$  but remain lower than the MF values in the scale free regime ( $\alpha \leq 3$ ). In BTW, the nodes with higher degree sustain large number of sand grains and play a role of reservoirs whereas in PSM no nodes of any degree sustain large number of sand grains, hence, such reservoirs do not exist. On the other hand, in MF analysis loop less structures in the branching process, nodes without multiple toppling, are assumed. Hence, the distributions  $P_s$  and  $P_a$  are characterized by the same exponents  $\tau_s = \tau_a$  and  $D_s = D_a$ . Thus the network structure (scale free or random) plays a crucial role in determining the critical behaviour of PSM in contrary to SSM.

It is now important to verify the effect of the choice of  $\epsilon$  on the scaling behaviour of PSM for a given  $\alpha$ . The distributions  $P_s(\alpha, q)$  and  $P_a(\alpha, q)$  for three different values of  $\epsilon$  are obtained and shown in Figs. 7(a) and 7(b) respectively for  $\alpha = 2.25$ . The cutoff of the distributions are found to depend on  $\epsilon$  as expected. Estimates of  $\sigma_s(\alpha, q)$  and  $\sigma_a(\alpha, q)$  are made for all three values of  $\epsilon$  at  $\alpha = 2.25$ . Variation of  $\sigma_s(\alpha, q)$  and  $\sigma_a(\alpha, q)$  against  $q$  are shown in Figs. 7(c) and 7(d) respectively. First of all the value of  $\sigma_s(1)$  for  $q = 1$  are found to increase as the value of  $\epsilon$  decreases as expected. Secondly, the plots intersect the  $q$ -axis at a single point. Since the  $q$  intercepts are  $\tau_s - 1$  or  $\tau_a - 1$ , the scaling exponents  $\tau_s$  or  $\tau_a$  remain independent of the choice of  $\epsilon$ . For  $\alpha = 2.25$ , the

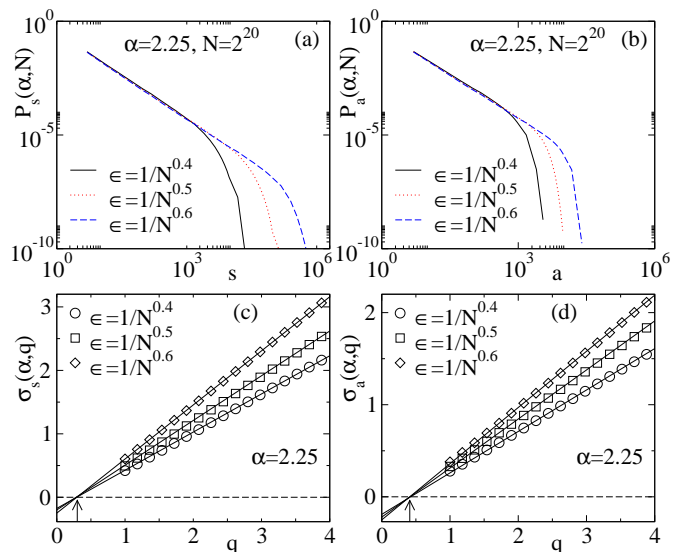


FIG. 7. (Colour online) Plot of (a)  $P_s(\alpha, N)$  and (b)  $P_a(\alpha, N)$  for  $\epsilon = 1/N^{0.4}$  (black solid line),  $\epsilon = 1/N^{0.5}$  (red dotted line), and  $\epsilon = 1/N^{0.6}$  (blue dashed line) for a fixed value of  $\alpha = 2.25$  and  $N = 2^{20}$ . Plot of (c)  $\sigma_s(\alpha, q)$  and (d)  $\sigma_a(\alpha, q)$  against  $q$  for  $\epsilon = 1/N^{0.4}$  ( $\circ$ ),  $\epsilon = 1/N^{0.5}$  ( $\square$ ), and  $\epsilon = 1/N^{0.6}$  ( $\diamond$ ). The solid lines represent the linear least square fit through the data points. The intersection points of the fitted lines are marked by arrow heads on the  $q$ -axis. The dashed lines correspond to  $\sigma_x = 0$ . For clarity points for  $q < 1$  are also dropped.

estimated values of  $\tau_s$  and  $\tau_a$  for  $\epsilon = 1/N^{0.4}$  and  $1/N^{0.6}$  are found to be within the error bar of the corresponding value of  $\tau_s$  and  $\tau_a$  for  $\epsilon = 1/N^{0.5}$ . However, the slope of the plots are found strongly dependent on  $\epsilon$ . Since the slope determines the capacity dimension  $D_x$ , it should depend on  $\epsilon$  for a given  $\alpha$ . For  $\alpha = 2.25$ , the values of  $D_s$  are found to be  $0.610(5)$  and  $0.857(4)$  for  $\epsilon = 1/N^{0.4}$  and  $1/N^{0.6}$  respectively and are out of the error bars of the corresponding value of  $D_s = 0.720(6)$  for  $\epsilon = 1/N^{0.5}$ . A similar result is also observed for  $D_a$ . Such dependence of the critical exponents on the choice of the dissipation factor is also reported in few other studies [22, 32].

It can be noted here that the results of PSM obtained here on the uncorrelated SFNs. The results have also been verified for correlated Barabasi-Albert SFN with  $\alpha = 3$ , generated by preferential attachment method [33] and the distributions  $P_s$  and  $P_a$  are found similar to those of PSM on the corresponding uncorrelated SFN with  $\alpha = 3$ . However, the SSM on optimized Barabasi-Albert SFN imposed on two dimensional square lattice with degree exponent  $\alpha = 3$  exhibits scaling behaviour with exponent  $\tau_s = 1.30$  [32]. A similar result is also obtained in the study of BTW type sandpile model on geographically embedded SFNs [34]. This is because of the fact that the optimization process destroys the small-world behavior though the degree distribution remains scale-free.

The scaling behaviour of  $P_x(\alpha, N)$  are found to be independent on the choice of  $k_{\max}$ , the cutoff degree of the

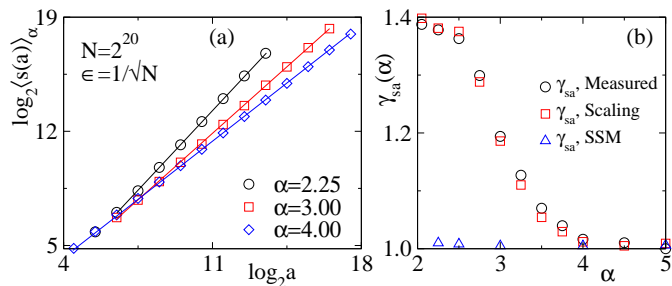


FIG. 8. (Colour online) (a) Plot of  $\langle s(a) \rangle_\alpha$  against  $a$  on a network of size  $N = 2^{20}$  with  $\epsilon = 1/\sqrt{N}$  for  $\alpha = 2.25$  ( $\circ$ ),  $\alpha = 3$  ( $\square$ ), and  $\alpha = 4$  ( $\diamond$ ). (b) Plot of  $\gamma_{sa}(\alpha)$  versus  $\alpha$ ; Circles represent the measured values of  $\gamma_{sa}$  and squares represent the same obtained from Eq. (8). Blue triangles in (b) represent  $\gamma_{sa}$  for the SSM.

network. It is also reported in the recent study of explosive percolation on SFN that the choice of cutoff degree of a network has little influence on the scaling behaviour of geometrical quantities [35].

Further insight can be obtained by studying the conditional expectation  $\langle s(a) \rangle_\alpha$  of the avalanche size  $s$  for a fixed area  $a$ . For a given  $\alpha$ ,  $\langle s(a) \rangle_\alpha$  expected to scale as

$$\langle s(a) \rangle_\alpha = \int sP(s|a)ds \sim a^{\gamma_{sa}(\alpha)}, \quad (7)$$

where  $P(s|a)$  is the conditional probability distribution and  $\gamma_{sa}(\alpha)$  is an exponent. The exponent  $\gamma_{sa}(\alpha)$  is expected to satisfy a scaling relation

$$\gamma_{sa}(\alpha) = \frac{\tau_a(\alpha) - 1}{\tau_s(\alpha) - 1} \quad (8)$$

with the exponents  $\tau_s(\alpha)$  and  $\tau_a(\alpha)$  as in usual sandpile models [15]. The exponent  $\gamma_{sa}(\alpha)$  is now measured and the scaling relation is verified. In Fig. 8(a),  $\langle s(a) \rangle_\alpha$  is plotted against  $a$  in double logarithmic scale for three different values of  $\alpha$  taking  $\epsilon = 1/\sqrt{N}$ . It can be seen that for a given  $\alpha$ ,  $\langle s(a) \rangle_\alpha$  scales with  $a$  as given in Eq. (7). Obtaining the slope by linear least square method through the data points, the values of  $\gamma_{sa}$  are measured and they are found as  $1.39 \pm 0.01$ ,  $1.19 \pm 0.01$ , and  $1.01 \pm 0.01$  for  $\alpha = 2.25$ , 3, and 4 respectively. The values of the exponent  $\gamma_{sa}(\alpha)$  are also measured for other values of  $\alpha$  and its variation with  $\alpha$  is shown in the Fig. 8(b). For  $\alpha \geq 4$ , not only the exponent  $\gamma_{sa} \approx 1$  but also the avalanche size  $s$  is equal to area  $a$ . This indicates that the nodes toppled only once during the avalanche and that is why the value of  $\tau_s$  is that of MF. Whereas, for  $\alpha < 4$ , the value of  $\gamma_{sa}$  is more than one and found to be  $\approx 1.4$  as  $\alpha \rightarrow 2$ . Not only the value of  $\gamma_{sa}$  is higher at a smaller  $\alpha$  than at a higher  $\alpha$ , the absolute value of avalanche size  $s$  is found to be higher for smaller values of  $\alpha$  at given avalanche area  $a$ . Thus, in the scale free regime ( $\alpha < 4$ ), a single node must have toppled multiple times to have higher avalanche size keeping avalanche area fixed. In order to verify the scaling relation given in Eq. (8), the

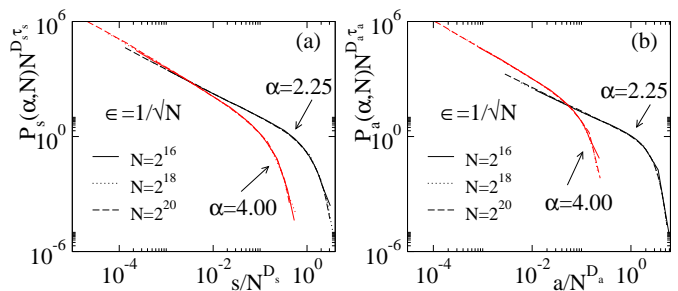


FIG. 9. (Colour online) Plot of  $P_x(\alpha, N)N^{D_x(\alpha)\tau_x(\alpha)}$  vs  $x/N^{D_x(\alpha)}$  for  $N = 2^{16}$  (solid line),  $N = 2^{18}$  (dotted line),  $N = 2^{20}$  (dashed line) for  $x = s$  in (a) and for  $x = a$  in (b) taking corresponding values of exponents. Distributions for  $\alpha = 2.25$  and for  $\alpha = 4$  are marked by arrows.

estimates of  $(\tau_a(\alpha) - 1)/(\tau_s(\alpha) - 1)$  are also plotted in Fig. 8(b) and compared with the directly measured value of  $\gamma_{sa}$ . It can be seen that the scaling holds within the error bars. As the exponents  $\tau_s$  and  $\tau_a$  are independent of dissipation factor  $\epsilon$ , the exponent  $\gamma_{sa}$  is also independent of  $\epsilon$ .

As the values of the critical exponents are found very different from those of the SSM in the scale free regime ( $\alpha < 4$ ), PSM then belongs to a new universality class than SSM in this regime of SFN. The results of the above model remain unchanged even if the two sand grains of a critical node goes randomly and independently to any of the highest and the lowest degree neighbouring nodes instead of giving one sand grain each to the highest and the lowest degree neighbouring nodes.

Knowing the values of the exponents  $\tau_x$  and  $D_x$  for a given  $\alpha$  and  $\epsilon$ , the scaling function form of  $P_x(\alpha, N)$  given in Eq. (4) is verified for both  $s$  and  $a$ . The scaled avalanche size distribution  $P_s(\alpha, N)N^{D_s(\alpha)\tau_s(\alpha)}$  is plotted against the scaled variable  $s/N^{D_s(\alpha)}$  in double logarithmic scales for three different network sizes  $N$  in Fig. 9(a) for  $\alpha = 2.25$  (in black) and  $\alpha = 4$  (in red) taking  $\epsilon = 1/\sqrt{N}$ . In Fig. 9(b), the scaled avalanche area distribution  $P_a(\alpha, N)N^{D_a(\alpha)\tau_a(\alpha)}$  is shown for the same values of  $\alpha$  and  $\epsilon$ . Using the respective values of the exponents, a good collapse of data are found to occur for both  $s$  and  $a$  irrespective of the values of  $\alpha$ . Hence, the FSS forms for  $s$  and  $a$  assumed in Eq. (4) are correct over the wide range of  $\alpha$  for a given  $\epsilon$ .

## VI. AUTO-CORRELATION IN TOPPLING WAVE

Since the model obeys FSS it is expected that there is no complete toppling balance in PSM. Complete toppling balance refers to the fact that the number of sands released by a toppled node is exactly equal to the number of sands received by it when each of its neighbour nodes topple once [36]. In PSM, if a node topples and gives sand to its highest and lowest degree neighbours

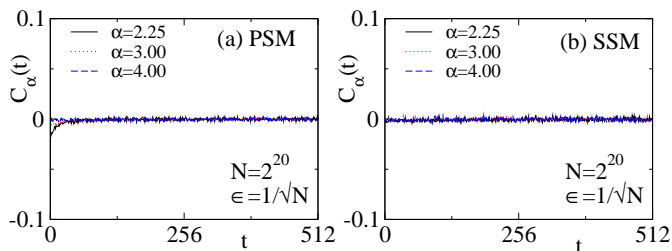


FIG. 10. (Colour online) Plot of  $C_\alpha(t)$  against  $t$  for  $\alpha = 2.25$  (black solid line),  $\alpha = 3$  (red dotted line), and  $\alpha = 4$  (blue dashed line) in (a) for PSM and in (b) for SSM.

it is not necessarily true that the toppled node is the highest or lowest degree node of any of the nodes those received sands. Hence, it is expected that such a toppling imbalance leads to the toppling waves generated from a fixed critical node to be uncorrelated. A toppling wave is the number of toppling during the propagation of an avalanche starting from a critical node without further toppling of the same node [37]. Each toppling of the critical node creates a new toppling wave. The avalanche size  $s$  can be considered as  $s = \sum_{j=1}^m s_j$ , where  $s_j$  is the size of the  $j$ th wave and  $m$  is the number of toppling waves in an avalanche. The time auto correlation [38] in the toppling waves on an SFN with given  $\alpha$  is defined as

$$C_\alpha(t) = \frac{\langle s_{j+t}s_j \rangle - \langle s_j \rangle^2}{\langle s_j^2 \rangle - \langle s_j \rangle^2}, \quad (9)$$

where  $t = 1, 2, \dots$  and  $\langle \dots \rangle$  represents the time average.  $C_\alpha(t)$  is calculated for both PSM and SSM on a network of size  $N = 2^{20}$  for several values of  $\alpha$  taking  $\epsilon = 1/\sqrt{N}$  and generating  $10^6$  toppling waves for each  $\alpha$ .  $C_\alpha(t)$  is plotted against  $t$  in Fig. 10 (a) for PSM and in Fig. 10 (b) for SSM. It can be seen that for both the models the values of  $C_\alpha(t)$  are always zero for different values of  $\alpha$ .

Hence, the toppling waves are completely uncorrelated as expected.

## VII. CONCLUSION

A two state sandpile model with preferential sand distribution is constructed and studied on scale free network varying the degree exponent  $\alpha$ . Due to the preferential constraint in the toppling rule, the sand grains upon toppling of a critical node go to the lowest and highest degree neighbour nodes. Such preferential sand distribution leads to entirely different avalanche evolution than that of the SSM in the scale free regime ( $\alpha < 4$ ) of the network. Employing moment analysis, various exponents have been estimated varying  $\alpha$ . For  $\alpha \geq 4$ , the exponents  $\tau_s$  and  $\tau_a$  become equal to  $3/2$ , the MF value whereas for  $\alpha < 4$ ,  $\tau_s < \tau_a < 3/2$  and has a continuous dependence on  $\alpha$  in contrary to the results of the SSM in which  $\tau_s = \tau_a = 3/2$  for the whole range of  $\alpha$ . The exponent  $\gamma_{sa}$  satisfies the scaling relation with  $\tau_s$  and  $\tau_a$  within error bars. All the distribution functions of the model satisfy FSS as there is no toppling balance and the time auto correlation in the toppling wave is vanishingly small. The PSM, sandpile model with preferential sand distribution, on SFN thus belongs to a new universality class than that of the SSM in the scale free regime of SFN.

**Acknowledgments:** This work is partially supported by DST, Government of India through project No. SR/S2/CMP-61/2008. Availability of computational facility, “Newton HPC” under DST-FIST project (No. SR/FST/PSII-020/2009) Government of India, of Department of Physics, IIT Guwahati is gratefully acknowledged.

- 
- [1] E. Ben-Naim, H. Frauenfelder, and Z. Toroczkai, *Complex Networks* (Springer-Verlag, Berlin, Heidelberg, Germany, 2004).
  - [2] M. E. J. Newman, *Networks: An Introduction* (Oxford University Press, Oxford, 2010).
  - [3] R. Albert and A.-L. Barabási, *Rev. Mod. Phys.* **74**, 47 (2002).
  - [4] R. Pastor-Satorras and A. Vespignani, *Phys. Rev. Lett.* **86**, 3200 (2001).
  - [5] R. M. May and A. L. Lloyd, *Phys. Rev. E* **64**, 066112 (2001).
  - [6] R. Cohen, D. ben Avraham, and S. Havlin, *Phys. Rev. E* **66**, 036113 (2002).
  - [7] A. L. Barabasi and H. E. Stanley, *Fractal concepts of surface growth* (Cambridge University Press, Cambridge, 1995).
  - [8] Z. Wu, C. Lagorio, L. A. Braunstein, R. Cohen, S. Havlin, and H. E. Stanley, *Phys. Rev. E* **75**, 066110 (2007).
  - [9] W. Wang, M. Tang, H. E. Stanley, and L. A. Braunstein, *Reports on Progress in Physics* **80**, 036603 (2017).
  - [10] R. Albert, H. Jeong, and A.-L. Barabasi, *Nature* **406**, 378 (2000).
  - [11] L. K. Gallos, R. Cohen, P. Argyrakis, A. Bunde, and S. Havlin, *Phys. Rev. Lett.* **94**, 188701 (2005).
  - [12] A. E. Motter and Y.-C. Lai, *Phys. Rev. E* **66**, 065102 (2002).
  - [13] M. L. Sachtjen, B. A. Carreras, and V. E. Lynch, *Phys. Rev. E* **61**, 4877 (2000).
  - [14] P. Bak, *How Nature Works: The Science of Self-Organized Criticality* (Copernicus, New York, 1996).
  - [15] H. J. Jensen, *Self-Organized Criticality* (Cambridge University Press, Cambridge, 1998).
  - [16] G. Pruessner, *Self-Organized Criticality: Theory, Models and Characterization* (Cambridge University Press, Cambridge, 2012).
  - [17] S. S. Manna, *Physica A* **179**, 249 (1991).

- [18] D. Dhar and R. Ramaswamy, Phys. Rev. Lett. **63**, 1659 (1989).
- [19] S. B. Santra, S. R. Channu, and D. Deb, Phys. Rev. E **75**, 041122 (2007).
- [20] P. Bak, C. Tang, and K. Wiesenfeld, Phys. Rev. Lett. **59**, 381 (1987).
- [21] P. Bak, C. Tang, and K. Wiesenfeld, Phys. Rev. A **38**, 364 (1988).
- [22] K.-I. Goh, D.-S. Lee, B. Kahng, and D. Kim, Phys. Rev. Lett. **91**, 148701 (2003).
- [23] D.-S. Lee, K.-I. Goh, B. Kahng, and D. Kim, Physica A: Statistical Mechanics and its Applications **338**, 835 (2004); K.-I. Goh, D.-S. Lee, B. Kahng, and D. Kim, Physica A: Statistical Mechanics and its Applications **346**, 936 (2005).
- [24] M. Catanzaro, M. Boguñá, and R. Pastor-Satorras, Phys. Rev. E **71**, 027103 (2005).
- [25] H. Bhaumik and S. B. Santra, Phys. Rev. E **88**, 062817 (2013).
- [26] S. S. Manna, J. Phys. A **24**, L363 (1991).
- [27] D. Dhar, Physica A **263**, 4 (1999), and references therein.
- [28] S. Lübeck, Phys. Rev. E **61**, 204 (2000).
- [29] E. Bonabeau, Journal of the Physical Society of Japan **64**, 327 (1995).
- [30] K. Christensen and Z. Olami, Phys. Rev. E **48**, 3361 (1993).
- [31] H. Bhaumik and S. B. Santra, Phys. Rev. E **94**, 062138 (2016).
- [32] R. Karmakar and S. S. Manna, J. Phys. A. **38**, L87 (2005).
- [33] A.-L. Barabási, R. Albert, and H. Jeong, Physica A: Statistical Mechanics and its Applications **272**, 173 (1999); A.-L. Barabási and R. Albert, Science **286**, 509 (1999).
- [34] L. Huang, L. Yang, and K. Yang, Phys. Rev. E **73**, 036102 (2006).
- [35] Radicchi and S. Fortunato, Phys. Rev. Lett. **103**, 168701 (2009).
- [36] Karmakar, S. S. Manna, and A. L. Stella, Phys. Rev. Lett. **94**, 088002 (2005).
- [37] V. B. Priezzhev, D. V. Ktitarov, and E. V. Ivashkevich, Phys. Rev. Lett. **76**, 2093 (1996); D. V. Ktitarov, S. Lübeck, P. Grassberger, and V. B. Priezzhev, Phys. Rev. E **61**, 81 (2000).
- [38] M. DeMenech and A. L. Stella, Phys. Rev. E **62**, R4528 (2000); Physica A **309**, 289 (2002); A. L. Stella and M. DeMenech, Physica A **295**, 101 (2001).